Search for H dibaryon on the lattice

Zhi-Huan Luo[1,2], Mushtaq Loan[3] and Yan Liu[2]
[1] School of Physics and Engineering, Sun Yet-Sen University, Guangzhou 510275, P. R. China
[2] Department of Applied Physics, South China Agricultural University, Guangzhou 510642, P. R. China
[3] International School, Jinan University, Guangzhou 510632, P. R. China
(Dated: August 2, 2011)

We investigate the H-dibaryon, an $I(J^P) = 0(0^+)$ with $s = -2$, in the chiral and continuum regimes on anisotropic lattices in quenched QCD. Simulations are performed on modest lattices with refined techniques to obtain results with high accuracy over a spatial lattice spacing in the range of $a_s \sim 0.19 - 0.40$ fm. We present results for the energy difference between the ground state energy of the hexa-quark stranglet and the free two-baryon state from our ensembles. A negative energy shift observed in the chirally extrapolated results leads to the conclusion that the measured hexa-quark state is bound. This is further confirmed by the attractive interaction in the continuum limit with the observed H-dibaryon bound by 47 ± 37MeV.

PACS numbers: 11.15.Ha, 14.40.Lb, 12.38.Gc, 12.38.Mh

arXiv:1106.1945v6 [hep-lat] 1 Aug 2011

I. INTRODUCTION

Search for dibaryons is one of the most challenging theoretical and experimental problems in the physics of strong interaction. In the non-strange sector, only one dibaryon, the deuteron, is known experimentally. In the strange sector, on the other hand, it is still unclear whether there are bound dibaryons or dibaryon resonances. Among others, the flavor-singlet state (uuddss), the H-dibaryon, has been suggested to be the most promising candidate [1]. The H-dibaryon may also be a doorway to strange matter that could exist in the core of neutron stars and to exotic hyper-nuclei [2, 3]. A deeply bound H with the binding energy $B_H > 7$ MeV from the $\Lambda\Lambda$ threshold has been ruled out by the discovery of the double Λ nuclei [4]. The double-hypernucleus events have either more than one interpretation for the products or the possibility of production of excited states. The analysis of the events in [4] ignored the possibility that the single or double hypernucleus was produced in an excited state in which case the value of the binding energy would increase by the excitation energy. Thus there still remains a possibility of a shallow bound state or a resonance in this channel. Since the Bag Model prediction of a deeply bound H-dibaryon, with large binding energy of $O(100)$ MeV [5], many experiments have been triggered to look for this possible particle, but few of them have confirmed the existence of the H-dibaryon [6–10]. The experiments were inspired by the Skyrme model prediction, and the experimental discoveries have in turn spawned intense interest on the theoretical side, with studies ranging from chiral soliton and large N_c models, quark models, phase-shift analysis and QCD sum rules [11]. Summarizing the previous theoretical and experimental investigations a slightly bound or unbound H-dibaryon is predicted.

In the search for such exotic states lattice QCD plays an important role in which precise predictions for hadronic observables with quantifiable uncertainties are made. A considerable interest in H-dibaryon started with Jaffe's work [5] demonstrating the role of the chromomagnetic interaction in the stability of light multiquarks. Since then a number of quenched LQCD calculations have been performed for the search of the H-dibaryon but no definite conclusions have been reported. Earlier lattice investigations [12, 13] gave somewhat mixed and contradicting results on the spatially localized resonance status of H-dibaryon. These studies however, suffered from low statistics, relatively large quark masses and considerable finite-size effects could not be rules out for the smaller lattice size. More precise studies on large volumes concluded an unbound H-dibaryon in infinite volume limit [14–16] while others reported hints of a bound H-dibaryon for a range of light-quark masses [17].

Very recently, NPLQCD and HALQCD Collaborations reported results from their fully dynamical lattice calculation that shed new light on the status of H-dibaryon [18, 19]. NPLQCD Collaboration presented a strong evidence for a bound H-dibaryon from their calculations performed in four lattice volumes. Using Lusher method [20] to extract two-particle scattering amplitude below threshold, NPLQCD collaboration found H-dibaryon bound by 16.6 MeV at a pion mass of $m_\pi = 390$ in the infinite volume limit [18]. Using their recently proposed approach of baryon-baryon potential [21], the HALQCD Collaboration performed calculations in three lattice volumes at three different quark masses and reported a bound H-dibaryon with the binding energy of $30 - 40$ Mev for the pion mass of $673 - 1015$ MeV [19]. These calculations provide strong evidence of capability of Lattice QCD in calculating the energy of simple nuclei, with H-dibaryon being an example. Having said that, it still remains an open question whether the H-dibaryon is bound at the physical point and with the inclusion of the electroweak interactions. This provides a strong motivation for pursuing numerical calculations at smaller lattice spacings, and over a range of quark masses including those of nature.

The target of this work is to address the status of the

H-dibaryon by calculating the mass differences between the candidate H-dibaryon and the free two-baryon states in the continuum limit and at physical quark masses. Using some refined methods and techniques, we carry a multi-lattice spacing analysis at and near physical pion mass on improved anisotropic lattices with an attractive feature that with modest lattice sizes one can access large spatial volumes while having a fine temporal resolution. Rather than extracting the hadron mass from the ratio of two temporal nearest correlators, the Levenberg-Marquardt algorithm is adopted to solve the hyperbolic-cosine ansatz of hadron correlation functions. This is very useful in finding a larger temporal fit range, hence more clear signals for precise hadron masses. Continuum limit is also considered in this work which will provides a real physical picture of the H-dibaryon.

The rest of the paper is organized as follows. The technical details of the lattice simulations are discussed in Sec. II, where we outline the construction of the correlation functions from interpolating operators and the actions used in this study. This section also discusses the procedures of chiral and continuum extrapolations. The results are presented and discussed in Sec. III, where we attempt to take the chiral and continuum limits and address chiral, finite-spacing and quenching effects. This sets the stage for a discussion of lattice resonance signature of the H-dibaryon lying lower than two-Λ channel masses in the physical regime. Finally, we present our conclusions in Sec. IV.

II. SIMULATION DETAILS

A. Choice of Interpolating fields

The explicit construction of the operator for H-dibaryon requires the symmetrization of the colour and spinor indices of two triplets of quarks in order to obtain colour and spin singlet. Our choice for the appropriate operator is motivated by possible structure of H-dibaryon and based on the idea of diquark formulation and has the following form [22, 23]:

$$\begin{aligned} O_H(x) &= 3(udsuds) - 3(ussudd) - 3(dssduu) \\ (udsuds) &= 3\epsilon^{abc}\epsilon^{def}(C\gamma_5)_{\alpha\beta}(C\gamma_5)_{\gamma\delta}(C\gamma_5)_{\epsilon\phi} \\ &\quad \times \left[u^a_\alpha d^b_\beta s^c_\epsilon u^d_\gamma d^e_\delta s^f_\phi\right], \end{aligned} \tag{1}$$

where the roman letters denote the colour indices, greek letters represent the spinor indices and ϵ^{abc} the usual antisymmetric tensor defined over the range of their indices. Taking the symmetry properties of the ϵ-tensor and the $(C\gamma_5)$-matrix under the interchange of two indices into account, the H-dibaryon correlation function can be obtained from

$$C_H(\vec{x},t) = < O_H(\vec{x},t)O_H^\dagger(0) > . \tag{2}$$

The hadron masses M_h and M_Λ, needed to obtain the energy shift $\Delta E = E_h - 2m_\Lambda$, are calculated by the fitting the correlation functions with a multi-hyperbolic-cosine ansatz

$$C(t) = \sum_{i=0}^{n} A_i \cosh[m_i(T/2-t)], \tag{3}$$

where m_i is the effective mass of the ith excited state and A_i the amplitude corresponding to this state. The method of calculation is straightforward in principle, not differing essentially from the calculation of hadron masses. We determine the mass of the ground state for each particle, and the mass difference $\Delta M(H-2\Lambda)$ from the fit. In order to reduce the contaminations of the excited states, the maximum time separation is used to extract the results. This is achieved by adopting the Levenberg-Marquardt algorithm to solve this non-linear least-squares fit. The hyperbolic-cosine fits are performed over the time interval in which an acceptable value of the probability, used to estimate the goodness-of-fit of the data, is obtained. Considering the contribution of ground state only, the correlation function is fitted by the form

$$C(t) = A_0 \cosh[m_0(T/2-t)]. \tag{4}$$

To account for the strong correlation of data in time, we use the full covariance matrix to construct the χ^2 function

$$\chi^2 = \sum_{i,j}[C(t_i,A_0,m_0) - D(t_i)]M^{-1}_{ij}[C(t_j,A_0,m_0) - D(t_j)], \tag{5}$$

and obtain the the covariance matrix M_{ij} as

$$M_{ij} = \frac{1}{N_c(N_c-1)}\sum_{k=1}^{N_c}[D(k,t_i) - D(t_i)][D(k,t_j) - D(t_j)], \tag{6}$$

where the $D(k,t_i)$ is the kth correlator and $D(t_i)$ the mean value of the correlator at time t_i, N_c denotes the total number of configurations. At minimum χ^2, the gradient of χ^2 with respect to the parameters (A_0, m_0) will be zero and the mass of ground state m_0 is estimated.

B. Anisotropic Lattice Actions

To examine the H-dibaryon in lattice QCD, we explore the improved actions on anisotropic lattices. These action display nearly perfect scaling, thus lattice-spacing artifact contributions are expected to be small, and providing reliable continuum limit results at finite lattice spacings can be obtained. With most of the finite-lattice artifacts having been removed, one can use coarse lattices with fewer sites and much less computational effort. Using a tadpole-improved anisotropic gauge action [24], we generate quenched configurations on a $12^3 \times 60$ lattice at five couplings in the range $\beta = 2.0 - 4.0$ and at a bare anisotropy of $\xi = 5.0$. We generated 500 gauge field

configurations for each lattice and the configurations are separated by 100 compound sweeps after skipping 1000 sweeps for the thermalization. We define a compound sweep as 5 over-relaxation [25] sweeps followed by one Cabbibo-Marinari [26] sweep.

For the fermion fields, we employ the space-time asymmetric clover quark action on anisotropic lattice [27, 28] with spatial Wilson parameter $r_s = 1$. The clover improvement coefficients $c_{s,t}$ are estimated from tree-level tadpole improvement whereas for the ratio of hopping parameters $\zeta = K_t/K_s$ we adopt both the tree-level improved value and a non-perturbative one. Since it becomes harder to obtain a reasonable signal-to-noise ratio at lighter quark masses for the multi-quark systems, we employ relatively heavy quark masses in our calculations. The bare strange quark mass is set by measuring the $s\bar{s}$ pseudoscalar mass at four heavy quark hopping parameters κ_h. At each strange quark mass, hadron propagators are measured for six light hopping parameters κ_l such that the mass ratio of M_K/M_N compares well with the experimental value. Our quenched quark propagators cover a range of quark masses, corresponding to pion masses from 1325 MeV down to 500 MeV. We also considered two smaller masses, but find that the signal for these becomes highly unstable, hence do not include these in our analysis.

C. Smearing technique

To increase the overlap of the operators with the ground state, all of the hadronic correlators were calculated using the method of smearing the interpolating operator, essentially making the hadronic operator spread around their central location in space. In this study, we use the gaussian smearing which is obtained by replacing the quark field $q(x)$ by the smeared quark field $q_{smear}(x)$ defined as [29]

$$q_{\rm smear}(t,\vec{x}) = N\sum_{y}\exp\{-\frac{|\vec{x}-\vec{y}|^2}{2\rho^2}\}q(t,\vec{y}), \qquad (7)$$

where N is an appropriate normalization factor and ρ the smearing size parameter. This technique has numerical advantages since the smearing function separates into two factors one belonging to the quark and the other to the antiquark, thus will help to maximize the ground state contribution relative to the ones of the excited states. The problem is that the smeared operators are no longer gauge-invariant because the quark and the antiquark are spatially separated. We employed Coulomb gauge fixing to overcome this problem.

D. Extrapolation to the physical quark mass and Continuum limits

Chiral extrapolations of the H-dibaryon mass and binding energy to the physical point are important issues. In the exact SU(3) flavour symmetry, the non-interacting $I(J^P) = 0(0^+)$ with strangeness $s = -2$ ground state is multiple degenerate, comprised of the states $\Lambda\Lambda$, $N\Xi$ and $\Xi\Xi$ with H-dibaryon as the ground state. A tightly bound H-dibaryon would indicate the chiral expansion of the form of that for single hadrons. The chiral extrapolation of single hadrons, such as the lowest-lying octet baryon masses, is an ongoing topic of discussion and motivates a deeper understanding of extrapolation form. The baryon chiral perturbation theory seems reluctant to reproduce LQCD results for the octet baryon masses, including the results for nucleon mass. Leinweber *et al* [30] demonstrated that the chiral extrapolation method based upon finite-range regulator leads to extremely accurate value for the mass of physical nucleon with systematic errors of less than one percent.

To addressed the challenges of SU(3) chiral perturbation theory to describe the baryon masses, Walker-Loud *e*t al., detailed a comprehensive chiral extrapolation analysis of the octet and decuplet baryon masses, using both the continuum SU(3) heavy baryon χPT as well as its mixed action generalization [31, 32]. The results placed signature of linearity of nucleon mass in m_π, providing a remarkable agreement with both the lattice data as well as the physical nucleon mass. This is in contrast with the expectations of chiral limit expansion of the general form $M_N(m_\pi) = a + bm_\pi^2 + O(m_\pi^3)$, where a and b are parameters determined from the lattice QCD data. Sharpe and Labrenz [33] also found a more complicated and available form of chiral expansion of baryon masses in quenched approximation. The problem is that we have only several binding energy for each lattice spacing, using the form made by Sharpe and Labrenz with so many coefficients may provides an unavailable and unreliable fit. Considering the form of binding energy is not known yet, we apply the general one to perform the chiral extrapolation and in fact we obtain a good result.

To avoid the ambiguity in the chiral limit estimates, we extrapolate mass difference and $\Delta M = M_H - 2M_\Lambda$ and mass ratios $\Delta M/M_\Lambda$ using the simplest ansatz consistent with leading order chiral effective theory,

$$f = \alpha + \beta x, \qquad (8)$$

where x represents the pion mass squared and α and β are fit parameters. The quantities f and x are accompanied by statistical errors. We intend to find the combination of α and β which minimizes

$$\sum_i \frac{\big(f(\alpha,\beta;x_i) - \langle f_i\rangle\big)^2}{\sigma_{f_i}^2 + \beta^2\sigma_{x_i}^2}, \qquad (9)$$

where i indexes different data points $\{x, f\}$ and σ is the statistical error of each quantity. The extrapolation is taken to physical point at fixed strange mass and M_Λ is taken as experimental input to make physical predictions.

The continuum extrapolation for the chirally extrapolated quantities is another important issue in lattice calculations. The possible error that might effect the simulation results comes from the scaling violation for our

action. Expecting that dominant part of scaling violation is largely eliminated by tadpole-improvement, we adopt an a_s^2-linear extrapolation to the continuum limit, since the lattice-spacing artifacts in our calculations are expected to scale as $O(a_s^2)$. Also, since the $O(a_s^2)$ effects largely cancel in forming the binding energy, we expect such contributions to be small.

III. RESULTS AND DISCUSSION

Typical examples of the effective mass plot at $(\kappa_l, \beta) = (0.3110, 3.60)$ and $(0.3115, 4.00)$ are shown in Fig. 1. As can be seen, smearing improves the overlap with the H-dibaryon ground state resulting in an earlier plateau. Consequently the contributions of excited states were substantially reduced. We find clear signals up to larger time separations with insignificant statistical fluctuation domination. The fit range $[t_{min}, t_{max}]$ is determined by fixing t_{max} and finding a range of t_{min} where the ground state is stable against t_{min}. The statistical error analysis is performed by a single-elimination jackknife method and the goodness of the fit is gauged by the χ^2 per degree of freedom, chosen according to criteria that χ^2/N_{DF} is preferably close to 1.0. The resulting effective masses of H-dibaryon and Λ states for other values of $a_t m_\pi$ at $\beta = 3.60$ are tabulated in Table I.

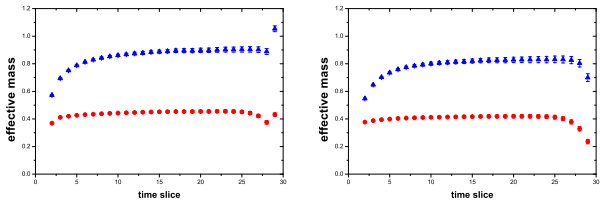


FIG. 1: Effective masses of the $I(J^P) = 0(0^+)$ stranglet (solid triangles) and lambda baryon (solid circles) at $(\kappa_l, \beta) = (0.3110, 3.60)$ (left panel) and $(\kappa_l, \beta) = (0.3115, 4.00)$ (right panel).

TABLE I: Effective masses of lambda baryon and H-dibaryon on the $12^3 \times 60$ lattice at $\beta = 3.60$ for various values of $a_t m_\pi$.

$a_t m_\pi$	$a_t M_\Lambda$	$a_t M_h$
0.38847(77)	0.5202(24)	1.0320(71)
0.36661(78)	0.4979(24)	0.9865(71)
0.34327(78)	0.4746(24)	0.9386(72)
0.31759(77)	0.4489(24)	0.8868(72)
0.28848(77)	0.4199(24)	0.8287(73)
0.25438(77)	0.3861(24)	0.7606(73)

In order to determine the energy difference $\Delta M = M_h - 2M_\Lambda$ precisely, we work in a regime where t is small enough that $t\Delta M << 1$, and at the same time t is large enough that the contributions of excited states are suppressed. Using the Levenberg-Marquardt algorithm, we indeed found such a range of t where linear term suffices in the data presented here. Fig. 2 shows the mass splitting between the H-dibaryon and 2Λ threshold for the parameter combination $(0.3110, 0.3115)$ at $a_s = 0.211$ and 0.188 fm, respectively. In the time interval where a single state dominates, the plateau region is reasonably consistent with that obtained for the effective mass of the H-dibaryon. The energy gap shows the negative value in the plateau region of $12 \leq t \leq 22$ and seems more pronounced with H-mass smaller than two Λ's. The signal of mass difference is dominated by the large fluctuations in the H-dibaryon correlators beyond $t \simeq 22$.

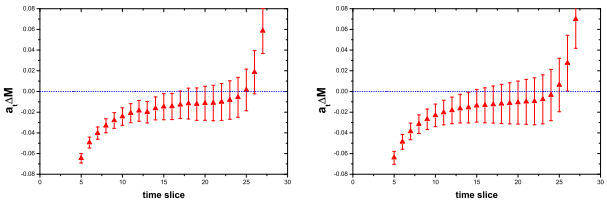


FIG. 2: Effective mass difference between the H-dibaryon state and the S-wave $\Lambda + \Lambda$ two-particle state at $(\kappa_l, \beta) = (0.3110, 3.60)$ (left panel) and $(\kappa_l, \beta) = (0.3115, 4.00)$ (right panel).

The results on the other lattice spacings shows consistency in the behaviour of mass difference over the range of our pion mass range (see Tables II, III and IV).

TABLE II: Mass differences and mass ratios between the H-dibaryon and $(\Lambda + \Lambda)$ two-particle state for various values of $a_t m_\pi$ at $\beta = 2.00$.

$a_t m_\pi$	$a_t \Delta M$	$\Delta M / M_\Lambda$
0.57298(32)	-0.0351(45)	-0.0396(51)
0.55564(31)	-0.0348(42)	-0.0401(49)
0.53723(30)	-0.0319(44)	-0.0375(51)
0.51770(29)	-0.0335(43)	-0.0402(51)
0.49682(29)	-0.0331(42)	-0.0407(52)
0.47430(28)	-0.0312(42)	-0.0394(52)

With all prerequisites available to measure the energy shift of H-dibaryon relative to the 2Λ threshold, we display, in Fig. 3, the resulting mass differences extrapolated to physical quark mass value using the ansatz in Eq. (8). We note that slope of a linear fit in m_π^2 is slightly different at all lattice spacings. On the other hand, mass difference is almost constant and weakly dependent on quark mass. Nevertheless the results on all lattice spacings exhibit a negative value in the physical region. The negative mass difference observed in this region would imply an attractive interaction and hence a signature of H-dibaryon as a bound state.

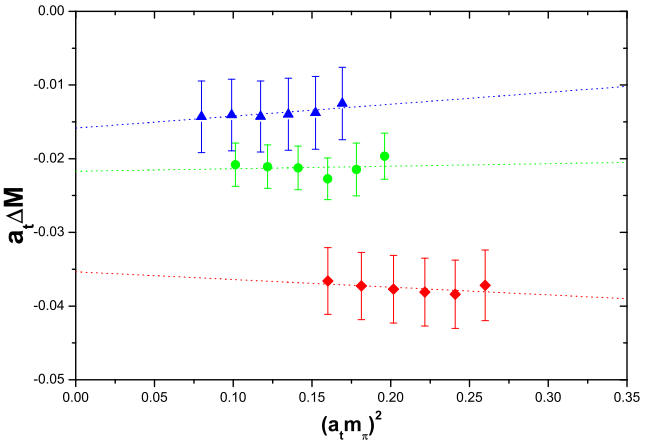


FIG. 3: Effective energy shift between the H-dibaryon state and $\Lambda + \Lambda$ two-particle state as a function of $a_t m_\pi$ squared. Solid circles, diamonds and triangles show the results at $\beta = 2.00, 2.80$ and 3.20, respectively.

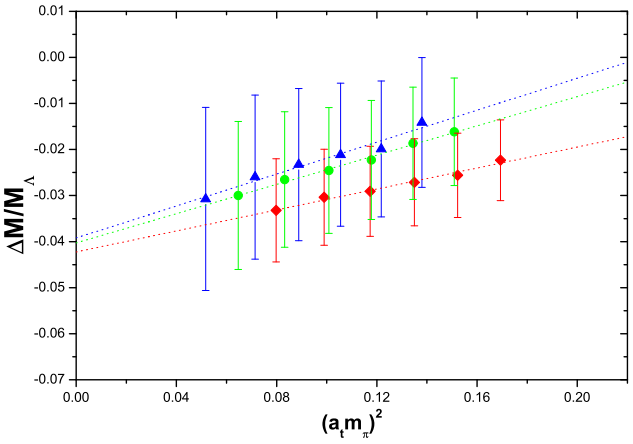


FIG. 4: Plot of mass ratio $\Delta M/M_\Lambda$ as a function of $a_t m_\pi$ squared. Solid circles, diamonds and triangles show the results at $\beta = 3.20, 3.60$ and 4.00, respectively. Dotted lines are the linear extrapolations to the chiral limit.

TABLE III: The same as Table II but at $\beta = 3.20$.

$a_t m_\pi$	$a_t \Delta M$	$\Delta M/M_\Lambda$
0.41147(45)	-0.0125(49)	-0.0223(87)
0.39017(46)	-0.0138(49)	-0.0256(92)
0.36742(46)	-0.0140(49)	-0.0271(94)
0.34252(46)	-0.0143(48)	-0.0291(98)
0.31463(46)	-0.0141(49)	-0.0304(104)
0.28250(47)	-0.0143(49)	-0.0332(112)

TABLE IV: The same as Table II, but at $\beta = 4.00$.

$a_t m_\pi$	$a_t \Delta M$	$\Delta M/M_\Lambda$
0.37144(91)	-0.0070(70)	-0.0141(141)
0.34893(91)	-0.0094(70)	-0.0199(148)
0.32486(90)	-0.0095(70)	-0.0211(155)
0.29802(89)	-0.0098(70)	-0.0233(165)
0.26725(88)	-0.0101(70)	-0.0260(178)
0.22738(111)	-0.0109(71)	-0.0307(199)

Since the quenched spectroscopy is quite reliable for mass ratio of stable particles, it is physically even more motivating to extrapolate mass ratio instead of mass. This allows for the cancellation of systematic errors since the hadron states are generated from the same gauge configuration and hence systematic errors are correlated. Fig. 4 shows the chiral extrapolation of the ratio $\Delta M/M_\Lambda$ at our smaller lattice spacings. The ratio shows a weaker dependence on quark mass and moves into the physical region with a trend of attractive interaction. In the chiral limit the estimated mass difference at our smallest and largest lattice spacings are consistent with those obtained by NPLQCD and HALQCD Collaborations [18, 19]. The uncertainties from the chiral fits range from 2 to 10 percent for to the smallest to largest lattice spacings explored here.

The quenching effects might be one of the largest source of the systematic uncertainties. However, with appropriate definition of scale, the mass ratios of stable hadrons differ from the corresponding observed values by less than 6% in quenched approximation [34, 35]. In order to absorb as many quenching effects as possible, we set the scale by the physical κ_s by calculating the ratio M_Λ/M_N. We found that the ratio deviates in the range of $3-4\%$ from its experimental value verifying that the value of κ_s used is very close to the physical quark mass. However, since our calculations use rather heavy pion masses (> 500 MeV), the quenching effects are less noticeable within our statistics. We include a modest estimate of order 5% quenching uncertainties in our analysis.

Whether the energy difference moves in the continuum with an attractive interaction needs to be explored. Since the finite-spacing errors in our calculations are expected to scale as a_s^2, we expect such contribution to have a small effect on binding energy. Consequently, we expect the observation of H-dibaryon to survive the continuum extrapolation. We perform the continuum extrapolation of the chirally extrapolated mass ratios in Fig. 5 and present the results in Table V. Using an a_s^2-linear extrapolation, we adopt the choice which shows the smoothest scaling behaviour for the final values, and use other to estimate the systematic errors.

As is clear from the figure, the mass ratio shows a weak dependence on the lattice spacing and varies only slightly over the fitting range. Thus we expect our continuum extrapolation accurate and unambiguous. The continuum extrapolation is accompanied with an order

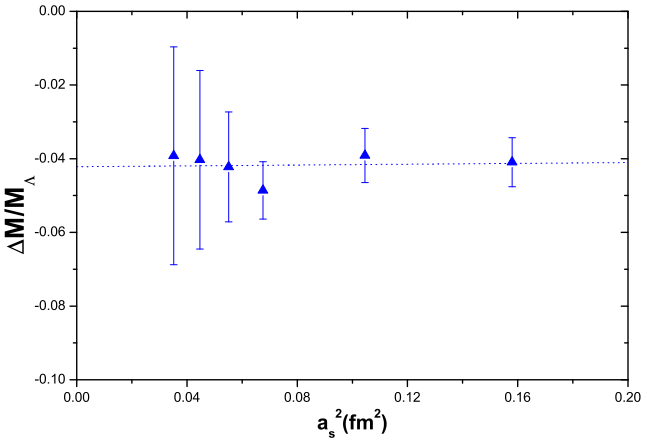


FIG. 5: Compilation of results for the mass ratio, $\Delta M/M_\Lambda$ in the continuum limit. The solid line represents a_s^2 linear extrapolation to the physical limit.

TABLE V: Mass ratios between the H-dibaryon and $(\Lambda + \Lambda)$ two-particle state at various lattice spacings.

a_s(fm)	$\Delta M/M_\Lambda$
0.3974(34)	-0.0409(66)
0.3234(43)	-0.0391(73)
0.2599(62)	-0.0486(78)
0.2347(57)	-0.0422(149)
0.2114(70)	-0.0403(242)
0.1875(56)	-0.0392(296)

8% systematic uncertainty from the linear fit in a_s^2. Using the physical Λ mass $M_\Lambda = 1115.68$ MeV, we obtain a continuum estimate of binding energy 47 ± 37 MeV for the binding energy. The uncertainty shown here results from the statistic and systematic uncertainties combined in quadrature. The systematic uncertainty including quenching, chiral and continuum extrapolation effects is estimated to be of the order of 15%. Note that we cannot estimate the finite size effects since we have been working with one lattice size. Even though our spatial extent of L is reasonably large, we cannot rule out the possibility of the volume dependence of the binding energy in the large volume limit. We intend to pin down this problem for a conclusive signature in future work.

IV. CONCLUSIONS

The question of whether the H-dibaryon is a bound or unbound state is still under debate. The observed negative energy shift pattern favours the former. In conclusion, we have presented evidence for existence of bound H-dibaryon state in the physical limit from quenched lattice QCD calculations. The calculations were performed over a range of pion masses and lattice spacings using improved anisotropic lattices with refined computational techniques. Attractive interaction was found in chiral limit for all pion masses used in this study and the continuum limit estimate seem to agree with the predicted value, which is one of the main results of our paper. Our results seem to be consistent with the recent results of NPLQCD and HALQCD Collaborations for the energy shift. Our analysis takes into account possible artifacts such as, statistical, chiral and continuum extrapolation uncertainties and those arising from quenching effects. On the basis of our lattice calculation we speculate that the H-dibaryon is to be identified as bound state. However, the final conclusions will have to await dynamical simulations incorporating a systematic study of various possible interpolators that are likely to have a good overlap with H-dibaryon. We plan to further develop this calculation to involve a combination of $\Lambda\Lambda - \Xi\Xi - \Sigma\Sigma$ interpolators on larger volumes.

V. ACKNOWLEDGEMENTS

ZHL is grateful to Professor Qiong-Gui Lin for discussions and valuable suggestions. This work is supported in part by the National Natural Science Foundation of China (Grant No. 11047021). ML is supported in part by the Department of Foreign Academic Affairs of Jinan University. We would like to express our gratitude to the Theoretical Physics Group at Sun Yat-Sen University for the access to its computing facility.

[1] E. Farhi and R. L. Jaffe, Phys. Rev. D **30**, 2379 (1984).
[2] C. Greiner and J. Schaffner-Bielich, nucl-th/9801062.
[3] C. Alcock, E. Farhi and A. Olinto, Nucl. Phys. (Proc. Suppl.) **B21**, 92 (1991).
[4] H. Takahashi *et al.*, Phys. Rev. Lett. **87**, 212502, (2001).
[5] R. Jaffe, Phys. Rev. Lett. **38**, 195 (1977).
[6] B. A. Shahbazian, V. A. Sashin, A. O. Kechechyan and A. S. Martynov, Phys. Lett. **B235**, 208 (1990).
[7] B. A. Shahbazian, T. A. Volokhovskaya, V. N. Yemelyanenko and A. S. Martynov, Phys. Lett. **B316**, 593 (1993).
[8] Yemelyanenko, A. S. Martynov and V. S. Rikhvitzkiy, Nucl. Phys. B (Proc. Suppl.) **75**, 63 (1999).
[9] A. Trattner, PhD Thesis, LBL, UMI-32-54109 (2006).
[10] C. Yoon *et al.*, Phys. Rev. C **75**, 022201 (2007).
[11] T. Sakai *et al.*, Prog. Theor. Phys. Suppl. **137**, 121 (2000).
[12] P. B. Mackenzie and H. B. Thacker, Phys. Rev. Lett. **55**, 2539 (1985).
[13] Y. Iwasaki, T. Yoshié, and Y. Tsuboi, Phys. Rev. Lett. **60**, 1371 (1988).

[14] J. W. Negele, A. Pochinsky and B. Scarlet, Nucl. Phys. B **73**, 255 (1999).
[15] I. Wetzorke, F. Karsch and E. Laermann, Nucl. Phys. B(Proc. Suppl.) **83**, 218 (2000).
[16] I. Wetzorke and F. Karsch, Nucl. Phys. B(Proc. Suppl.) **119**, 278 (2003).
[17] Z. Luo, M. Loan and X.Q. Luo, Mod. Phys. Lett. **A22**. 591 92007).
[18] S. Beane *et al.* [NPLQCD Collaboration], Phys. Rev. Lett. **106**, 162001 (2011).
[19] T. Inoue *et al.* [HAL QCD Collaboration], Phys. Rev. Lett. **106**, 162002 (2011)
[20] S. Beane *et al.* [NPLQCD Collaboration], Phys. Lett. B **585**, 106 (2004)
[21] N. Ishii, S. Aoki and T. Hatsuda, Phys. Rev. Lett. **99**, 022001 (2007)
[22] J. F. Donoghue, E. Golowich and B. R. Holstein, Phys. Rev. D **34**, 3434 (1986).
[23] E. Golowich and T. Sotirelis, Phys. Rev. D **46**, 354 (1992).
[24] C. J. Morningstar and M. Peardon, Phys. Rev. D **56**, 4043 (1997).
[25] M. Creutz, Phys. Rev. D **21**, 2308 (1980).
[26] N. Cabibbo and E. Marinari, Phys. Lett. B **119**, 387 (1982).
[27] M. Okamoto et al., Phys. Rev. D **65**, 094508 (2002).
[28] J. Harada, H. Matsufuru, T. Onogi and A. Sugita, Phys. Rev. D **66**, 014509 (2002).
[29] C. Bernard *et al.*, Nucl. Phys. B (Proc. Suppl.) 60A, 3-13 (1998).
[30] D. B. Leinweber, A. W. Thomas and R. D. Young, Phys. Rev. Lett. **92**, 242002 (2004).
[31] A. Walker-Loud, PoS **Lattice 2008**, 005 (2008).
[32] A. Walker-Loud, *et al.*, Phys. Rev. D **79**, 054502 (2009).
[33] J. N. Labrenz, and S. R. Sharpe, Phys. Rev. D **54**, 4595 (1996).
[34] F. Butler, H. Chen, J. Sexton, A. Vaccarino and D. Weingarten, Phys. Rev. Lett. **70**, 2849 (1993).
[35] A. Ali Khan *et al.* [CP-PACS Collaboration], Phys. Rev. D **65**, 054505 (2002).